Solvated Electron Pairing with Earth Alkaline Metals in THF 2−Reactivity of the (Mg^{II}, e$_s^-$) Pair with Aromatic and Halogenated Hydrocarbon Compounds

F. Renou, P. Pernot, J. Bonin, I. Lampre, and M. Mostafavi*

Laboratoire de Chimie Physique, CNRS UMR 8000, Université Paris-Sud, Centre d'Orsay, Bât. 349, 91405 Orsay Cedex, France

The reactivity of the pair formed by magnesium perchlorate with solvated electron in THF with aromatic molecules and halogenated hydrocarbons was investigated by pulse radiolysis. The kinetics of electron transfer from the pair to aromatic molecules with reduction potentials covering a 1 V range were recorded. The corresponding rate constants were determined and show that the pair presents a strong reducing character because it can reduce biphenyl which has a low redox potential. Nevertheless, the pair is still a weaker reducing agent than the solvated electron in THF. Moreover, we estimated the rate constants of the reaction between the pair and different types of alkyl halogenides.

I. Introduction

Some metal cations, such as alkaline and earth alkaline, cannot be reduced by hydrated electrons in water. Nevertheless, the reduction of alkaline metal cations by solvated electrons has been studied in less polar solvents.[1,2] In a previous pulse radiolysis study of the reactivity of solvated electron with divalent magnesium (Mg^{II}) salts in tetrahydrofuran (THF), we ascertained the formation of a pair involving Mg^{II} and solvated electrons in THF.[3] This reaction occurs when magnesium perchlorate salt is used but not in the case of magnesium chloride salt. Conductivity measurements revealed that the salts are not dissociated in THF solution, indicating that the solvated electron reacts with the uncharged form of the metal cation, Mg(ClO$_4$)$_2$, according to reaction 1

$$Mg(ClO_4)_2 + e_s^- \rightarrow [Mg(ClO_4)_2, e_s^-] \qquad (1)$$

The rate constant value of the above reaction was estimated to be $k_1 = (6.2 \pm 0.2) \times 10^9$ dm^3 mol^{-1} s^{-1}. The identification of the product of reaction 1 as a pair was derived from quantum chemistry calculations. We showed that it presents a specific absorption spectrum in the near-infrared domain with a band maximum located around 950 nm in THF.[3,4] We observed also that the pair disappears following a first-order kinetic law. The proposed mechanism for the decay of the pair involves two reactions, on one hand the dissociation of the pair according to reaction 2 (reverse of reaction 1)

$$[Mg(ClO_4)_2, e_s^-] \rightarrow Mg(ClO_4)_2 + e_s^- \qquad (2)$$
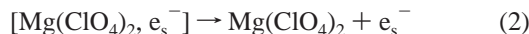
with a rate constant $k_2 = (3.8 \pm 0.1) \times 10^6$ s^{-1}, and on the other hand the probable internal reduction of the pair (reaction 3) leading to a species that does not absorb in the visible and near-infrared domain

$$[Mg(ClO_4)_2, e_s^-] \rightarrow MgO^+ (ClO_3^-)ClO_4^- \qquad (3)$$

with a rate constant $k_3 < 10^5$ s^{-1}. The latter channel of the pair decomposition is negligible. Moreover, we checked that a direct oxidation of the pair by solvent cation (THF$^+$) is too slow to be considered and the pair disappears mostly through the reaction 2.

In the present work, we study the reactivity of the pair, hereafter referred to as (Mg^{II}, e$_s^-$), in the presence of different organic solutes in THF, using the pulse radiolysis technique. We depict and analyze the signals showing the electron-transfer reactions from the pair to different aromatic molecules. From the determined rate constants, we derive an approximate limit for the redox potential of the pair. We also observe the reaction between alkyl halides RX and the pair. As a matter of fact, the reduction of halogenated hydrocarbons leading to the halide ion and a carbon-centered radical is often used in radiation chemistry to produce well-defined radicals because of the selective cleavage of the carbon−halogen bond by the attack of the solvated electron. Such a reduction, inducing a dehalogenation of hydrocarbon compounds, is also of great interest for environmental problems related to the destruction of halogenated organic contaminants in water and soil.[5] For instance, a process based on the magnesium hydrolysis in the presence of a platinum catalyst has been proposed to degrade halogenated compounds to low molecular weight hydrocarbons.[6] In other respects, the chemical behavior of the (Mg^{II}, e$_s^-$) pair toward the RX molecules should enable us to get a better understanding of the formation mechanism of Grignard reagents (RMgX). Indeed, the pair could be one of the transient species involved in the formation of organomagnesian compounds, and the knowledge of the reactivity between (Mg^{II}, e$_s^-$) and RX gives us the rate constant for one of the possible steps involved in the process of Grignard formation.[7]

II. Experimental and Theoretical Details

Tetrahydrofuran (THF) from Fluka (99.5% purity) was distilled over sodium metal under argon atmosphere to remove water and oxidizing agents. Magnesium perchlorate from Aldrich was used as received. Aromatic compounds, commercially supplied with a nominal purity around 95%, were used without further purification: biphenyl was purchased from

* To whom correspondence should be addressed. E-mail: mehran.mostafavi@lcp.u-psud.fr.

Aldrich; phenanthrene from Eastman Kodak; and chrysene, anthracene, and tetracene from Fluka. The alkyl halogen compounds with a purity of at least 98% were also used as received. Iodomethane (CH_3I), 1-chloropropane (C_3H_7Cl), 1-chlorobutane (C_4H_9Cl), and chloromethylbenzene ($C_6H_5CH_2$-Cl) were purchased from Aldrich. 1-Chloropentane ($C_5H_{11}Cl$), bromobenzene (C_6H_5Br), iodobenzene (C_6H_5I), and bromo-methylbenzene ($C_6H_5CH_2Br$) come from Fluka, whereas chloro-benzene (C_6H_5Cl) is from Prolabo.

The pulse radiolysis setup has been described elsewhere.[8] Electron pulses (3 ns duration) were delivered by a Febetron 706 accelerator (600 keV electron energy) to samples contained in a quartz suprasil cell through a thin entrance window (0.2 mm) having an optical path length (1 cm) perpendicular to the electron beam. The cell was deaerated by nitrogen flow before the experiment. The solution was changed after each pulse. The optical absorption of the transient species was recorded by means of a classical xenon lamp, monochromator, and photomultiplier or diode setup with a sensitive surface of 1 mm radius. The spectrophotometer detection system had an overall rise-time of 3.7 ns in the visible spectral domain and 12 ns in the infrared domain. The reported values of the optical density at different wavelengths are the average of at least 10 measurements.

The primary effects of the interaction of high energy radiation such as electron beam with THF solutions are the excitation and ionization of the solvent. Fast subsequent processes, solvation, dissociation of excited states, ion−molecule reaction, and radical−radical reaction lead to molecular and radical species able to recombine or react with the solute. Hereafter, THF^+ stands for the hole or radicals formed in the solution by the electron pulse that may recombine with the solvated electron.

The data analysis method of the time-resolved signals has been detailed in ref 3 and is implemented in a homemade program. The transient absorbance signal, $A(t,\lambda)$, is a function of time t and wavelength λ and is formulated as follows:

$$A(t,\lambda) = \sum_{i=1}^{n} c_i(t;\mathbf{K})\epsilon_i(\lambda) \qquad (4)$$

where $c_i(t;\mathbf{K})$ is the concentration of the species i at time t for a set of parameters involved in the kinetics model, $\mathbf{K}$, and $\epsilon_i(\lambda)$ is the molar extinction coefficient of the species i at a given wavelength λ. The posterior probability density function (pdf), $p(k|D)$, for the parameters k conditional to the dataset (signals) D is obtained in a Bayesian framework.[9] The posterior pdf depends on the prior pdf, $p(k)$, for the parameters and on the likelihood function $p(D|k)$ through Bayes' rule:
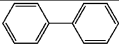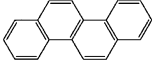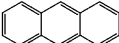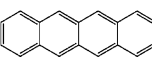
$$p(k|D) \propto p(D|k)\, p(k) \qquad (5)$$

The explicit expression of the likelihood function $p(D|k)$ has been shown in the appendix of the first paper of this series to be a function of the sum of the squares of residuals between the model and the data.[3] The optimal set of parameters (the best fit) corresponds to the maximum of the posterior pdf. Statistical estimates for the parameters or any function of them, $E[f]$, are obtained from the posterior pdf:

$$E[f] = \int dk\, f(k)\, p(k|D) \qquad (6)$$

The multidimensional integrations are actually performed by a Markov Chain Monte Carlo (MCMC) method.[10]

TABLE 1: Formula, Relative Reduction Potential^a of Aromatic Compounds and Rate Constant of Their Reaction with the (Mg^{II}, E$_s^−$) Pair in THF

Compound	Formula	$\Delta E°$ (V)	k (dm^3 mol^{-1} s^{-1})
Biphenyl		0	$(7.0 \pm 0.1) \times 10^9$
Phenanthrene		0.13 ± 0.01	$(8.6 \pm 0.4) \times 10^9$
Chrysene		0.30 ± 0.1	$(9.2 \pm 0.5) \times 10^9$
Anthracene		0.64 ± 0.02	$(1.3 \pm 0.1) \times 10^{10}$
Tetracene		1.06 ± 0.04	$(2.8 \pm 0.1) \times 10^{10}$

^{a} The reduction potential of the couples (Ar/Ar$^-$) in THF refer to that of biphenyl and are taken from ref 13 and 24, except the chrysene one which is estimated from the redox potentials of the series in 1,2-dimethoxyethane.[25] In the latter solvent, $E°(Ph_2/Ph_2^-) = -2.56$ V$_{NHE}$.[25]

The interest of this approach is manifold:

(1) diagnostic detection of identifiability problems;

(2) direct and accurate estimation of the uncertainties in the parameter values;

(3) elimination of nuisance parameters through marginalization;

(4) consistent use of a priori information through the prior pdf.

Simultaneous analysis of complementary signals (global analysis) is performed in order to enhance the identifiability of the kinetics parameters. In the present experimental conditions (i.e., in the absence of accurate dose rate and radiolytic yields for the precursor species), we have to consider two unknown parameters per signal (initial concentrations of e$_s^-$ and THF$^+$), in addition to the reaction rate constants and spectral properties of the different species. The increase in parameter number with the number of signals is detrimental to the efficiency of the MCMC calculations. Consequently, we adopt a mixed approach, using global analysis together with the facility of information transfer offered by the Bayesian framework, and limited sets of signals (designed to identify particular parameters) were analyzed successively instead of the full set at once.

The time dependent concentrations are obtained by numerical solutions of the kinetic differential equations (LSODA).[11]

III. Results and Discussion

III.1. Reactivity with Aromatic Compounds. To character-ize the redox properties of the (Mg^{II}, e$_s^-$) pair, we study the electron-transfer reaction between the pair and aromatic mol-ecules (Ar) with different reduction potentials (Table 1). Pulse radiolysis experiments have been carried out with THF solutions containing magnesium perchlorate and one aromatic compound. In the following sections, we present the full kinetics analysis that has been performed in the case of biphenyl to establish the optimal experimental conditions and the mechanism of the decay of the pair. The full kinetics analysis enables us also to validate a much simpler treatment, i.e., the pseudo-first-order kinetics analysis of the (Mg^{II}, e$_s^-$) signals in the presence of various electron acceptors. This pseudo-first-order analysis eventually has been used for the (Mg^{II}, e$_s^-$) decay in the presence of other compounds.

III.1.a. Radiolysis of THF Solution Containing Biphenyl. After the electron pulse irradiation of THF solutions containing magnesium perchlorate and biphenyl, there is a competition
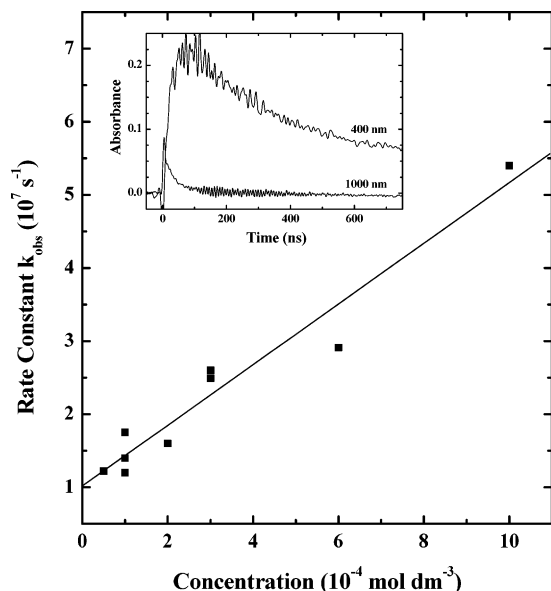
Reactivity of the (Mg^{II}, E$_s^-$) Pair

J. Phys. Chem. A, Vol. 107, No. 34, 2003 **6589**

Figure 1. First-order rate constant, k_{obs}, of the optical change observed at 1000 nm as a function of the biphenyl concentration in THF solution. Inset: Time profile of the transient absorption signals monitored at 400 and 1000 nm upon pulsed radiolysis of THF solution containing 3 × 10^{-4} mol dm^{-3} of biphenyl.

between the pair formation (reaction 1) and the electron scavenging by biphenyl

$$Ph_2 + e_s^- \rightarrow Ph_2^- \tag{7}$$

Inasmuch as we could not fit our data with the value of k_7 reported in the literature,[1,12] in order to be able to determine k_7, we have recorded transient signals for THF solutions containing only biphenyl at different concentrations, in the absence of magnesium perchlorate.

At 1000 nm, only the solvated electron absorbs because the biphenylide radical anion (Ph$_2^-$) absorbs in the visible domain.[13] Its absorption spectrum presents two bands peaking at 400 and 630 nm with molar extinction coefficients of 4 × 10^4 and 1.25 × 10^4 dm^3 mol^{-1} cm^{-1}, respectively.[13] As the extinction coefficient of the solvated electron at 400 nm is negligible, we have chosen to monitor the transient absorbance at 400 and 1000 nm. The signals for THF solution containing 3 × 10^{-4} mol dm^{-3} biphenyl are reported in the inset in Figure 1. We emphasize that the rise in the transient absorbance at 400 nm showing the appearance of Ph$_2^-$ is correlated to the decay of the solvated electron and reaches its maximum around 100 ns after the electron pulse, when the solvated electron vanishes. Then, the absorbance at 400 nm decreases slowly. The decay at 400 nm is complex as the radical anion reacts to form a species (Y) which absorbs around 400 nm. That species might be the radical Ph$_2$H$^\bullet$ issued from the reaction with the solvent cation (THF$^+$) as already observed in polar media (amines, alcohols, water)[14]

$$Ph_2^- + THF^+ \rightarrow Y \tag{8}$$

For the investigated biphenyl concentration range from 5 × 10^{-5} to 10^{-3} mol dm^{-3}, the decay of the solvated electron at 1000 nm follows a pseudo-first-order law with an observed rate constant k_{obs} (Figure 1). The linear fit of k_{obs} versus the biphenyl concentration gives a value of $k_7 = (4.1 \pm 0.4) \times 10^{10}$ dm^3 mol^{-1} s^{-1}. However, as the decay of the solvated electron is very fast and the experimental points are relatively scattered, we have performed a global analysis of a set of six signals

TABLE 2: Estimation of the Parameters^a from the Probabilistic Analysis of the Transient Signals Recorded at 400 nm upon Pulse Radiolysis of THF Solutions Containing Biphenyl

parameters	prior	posterior
k_7 (dm^{3}mol^{-1}s^{-1})	[10^8;10^{13}]	(3.9 ± 0.1) × 10^{10}
k_8 (dm^{3}mol^{-1}s^{-1})	[10^8;10^{13}]	(3.7 ± 0.2) × 10^{11}
k_9 (dm^{3}mol^{-1}s^{-1})	(1.9 ± 0.2) × 10^{12} ^{b}	(1.7 ± 0.1) × 10^{12}
$\epsilon_{e_s^-}$ (dm^{3}mol^{-1}cm^{-1})	0	
$\epsilon_{Ph_2^-}$ (dm^{3}mol^{-1}cm^{-1})	[10;10^5]	(3.9 ± 0.2) × 10^4
$\epsilon_Y(400)$ (dm^{3}mol^{-1}cm^{-1})	[10;10^4]	(3.6 ± 0.3) × 10^3

^{a} A single value x represents a dirac density function (fixed value of the parameter); m ± s summaries a normal density function of mode m and standard deviation s; [a;b] stands for a log-uniform density function between boundaries a and b. ^{b} Taken from ref 3.

monitored at 400 nm. In the kinetics simulations, we take into account reactions 7 and 8 as well as the overall recombination reaction

$$e_s^- + THF^+ \rightarrow products \tag{9}$$

We use as prior functions for k_9 the normal distribution previously obtained[3] and for all of the other parameters log uniform distributions (Table 2). A Markov chain of 5 × 10^5 steps initiated from the mode of the posterior pdf provides converged estimates for the 17 parameters (12 unknown initial concentrations and 5 kinetic and spectral parameters). The reaction rate constants k_7 and k_8 are found to be (3.9 ± 0.1) × 10^{10} and (3.7 ± 0.1) × 10^{11} dm^3 mol^{-1} s^{-1}, respectively. The extinction coefficients at 400 nm for the biphenylide ion and the absorbing species Y formed through reaction 8 are $\epsilon_{Ph_2^-}$(400) = (3.9 ± 0.2) × 10^4 and $\epsilon_Y(400)$ = (3.6 ± 0.3) × 10^3 dm^3 mol^{-1} cm^{-1}. The estimated value of $\epsilon_{Ph_2^-}$(400) is in excellent agreement with the literature value (4 × 10^4 dm^3 mol^{-1} cm^{-1}).[13] We note that the value of $\epsilon_{Ph_2^-}$(400) and its uncertainty depend on the value of $\epsilon_{e_s^-}$(1000) (assumed to be 10^4 dm^3 mol^{-1} cm^{-1} taken from ref 15) through the prior pdf used here for k_9 (see Table 1 in ref 3 and Table 2 of the present paper). The value of k_7 corroborates the estimation from the linear fit of k_{obs} (Figure 1). This value is nearly three times lower than the reported one, $k_7 = (1.1 \pm 0.3) \times 10^{11}$ dm^3 mol^{-1} s^{-1}.[1,12] The latter value was first determined by observing the appearance of Ph$_2^-$ at 630 nm where both the biphenylide ion and the solvated electron absorb.[1] Our value was deduced from signals, with a better time resolution, at two different wavelengths where only one of the species absorbs. Moreover, our value is in accordance with recent pulse radiolysis measurements showing that the reported value should be revised downward to around 5 × 10^{10} dm^3 mol^{-1} s^{-1}.[16]

III.1.b. Reactivity of the (Mg^{II}, e$_s^-$) Pair with Biphenyl. The reaction between (Mg^{II}, e$_s^-$) and biphenyl is investigated over a biphenyl concentration range from 10^{-4} to 10^{-3} mol dm^{-3} in THF solutions containing magnesium perchlorate. As the rate constant of the pair formation is relatively slow, there is a competition between the direct reaction of the solvated electron with the aromatic compounds and the formation of the pair. Consequently, in that study (and in the following sections), we fix the concentration of magnesium perchlorate at 10^{-2} mol dm^{-3}, in excess compared to the concentration of the organic solute to favor the formation of the (Mg^{II}, e$_s^-$) pair. We note also that in any studied solutions all solvated electrons are scavenged within the pulse. As an example, Figure 2 presents the time profile of the transient absorption signals monitored at 400 and 1000 nm upon pulse radiolysis of THF solution containing 10^{-2} mol dm^{-3} Mg(ClO$_4$)$_2$ and 5 × 10^{-4} mol dm^{-3}
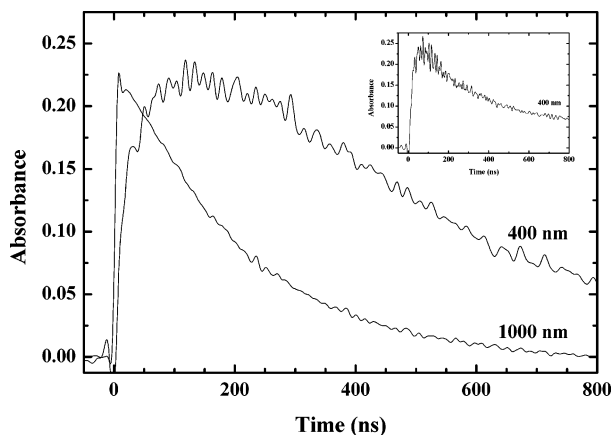
Figure 2. Time profile of the transient absorption signals monitored at 400 and 1000 nm upon pulsed radiolysis of THF solution containing 10^{-2} mol dm^{-3} of magnesium perchlorate and 5×10^{-4} mol dm^{-3} of biphenyl. Inset: Time profile of the transient absorption signals monitored at 400 upon pulsed radiolysis of THF solution containing only 5×10^{-4} mol dm^{-3} of biphenyl.

Ph$_2$. The signal at 400 nm shows the appearance of the biphenylide ion, whereas the absorption signal at 1000 nm is mainly due to the (Mg^{II}, e_s^-) pair.[3] Under the present experimental conditions, the (Mg^{II}, e_s^-) pair is mostly formed within the electron pulse duration leading to a very fast rise in the absorbance at 1000 nm. Thereafter, the pair disappears following pseudo-first-order decay (Figure 2).

The presence of Mg(ClO$_4$)$_2$ in solution significantly modifies the shape of the signal observed at 400 nm. In the absence of Mg(ClO$_4$)$_2$, we observe a fast rise in the absorbance until 50 ns followed by a slow decay (Figure 2 inset). In the presence of 10^{-2} mol dm^{-3} Mg(ClO$_4$)$_2$ the signal at 400 nm consists of three parts, first a very fast increase (because of the direct reduction of biphenyl through the reaction 7) within the electron pulse duration, then a supplementary rise in the absorbance reaching a maximum around 150 ns and eventually a slow decay lasting few hundreds of nanoseconds (Figure 2). The slow supplementary growth of the absorbance at 400 nm after the electron pulse, indicating a subsequent formation of Ph$_2^-$, is correlated to the decay of the pair at 1000 nm. We conclude that an electron transfer occurs from the (Mg^{II}, e_s^-) pair toward the biphenyl to produce the biphenylide ion according to reaction 10

$$(Mg^{II}, e_s^-) + Ph_2 \rightarrow Ph_2^- + Mg^{II} \qquad (10)$$
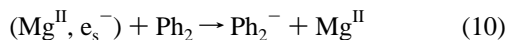
It is known that biphenylide or pyrenide ions can form ion pairs with sodium cations.[17,18] Consequently, the biphenyl radical anion might form such a pair with the metal cation leading to an association equilibrium

$$Ph_2^- + Mg^{II} \rightarrow (Mg^{II}, Ph_2^-) \qquad (11)$$

$$(Mg^{II}, Ph_2^-) \rightarrow Ph_2^- + Mg^{II} \qquad (12)$$
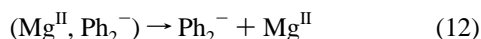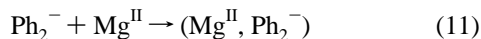
In the kinetics model used for the global analysis of five transient signals recorded at 1000 nm over the whole biphenyl concentration range, nine reactions are considered: reactions 1−3 and 7−12. For the rate constants of reactions 7 and 8, we use as prior functions (prior in Table 3) the posterior distributions determined above (posterior in Table 2). The prior functions for the rate constants of reactions 1, 2, 3, and 9, and for the molar extinction coefficients at 1000 nm of the solvated electron, $\epsilon_{e_s^-}$ (1000), and the pair $\epsilon_{(Mg^{II}, e_s^-)}$(1000) are the posterior distributions taken from ref 3. Four global parameters are

TABLE 3: Estimation of the Parameters^a from the Probabilistic Analysis of the Transient Signals Recorded at 1000 nm upon Pulse Radiolysis of THF Solutions Containing Biphenyl and Magnesium Perchlorate

parameters	prior	posterior
k_1 (dm^{3}mol^{-1}s^{-1})	$(6.2 \pm 0.2) \times 10^{9\ b}$	$(6.1 \pm 0.2) \times 10^9$
k_2 (s^{-1})	$(3.8 \pm 0.1) \times 10^{6b}$	$(3.8 \pm 0.1) \times 10^6$
k_3 (s^{-1})	$10^{4\ b}$	
k_7 (dm^{3}mol^{-1}s^{-1})	$(3.9 \pm 0.1) \times 10^{10\ c}$	$(3.9 \pm 0.1) \times 10^{10}$
k_8 (dm^{3}mol^{-1}s^{-1})	$(3.7 \pm 0.2) \times 10^{11\ c}$	$(3.7 \pm 0.2) \times 10^{11}$
k_9 (dm^{3}mol^{-1}s^{-1})	$1.9 \times 10^{12\ b}$	
k_{10} (dm^{3}mol^{-1}s^{-1})	$[10^8; 10^{10}]$	$(7.0 \pm 0.1) \times 10^9$
$\epsilon_{e_s^-}$ (dm^{3}mol^{-1}cm^{-1})	$10^{4\ b}$	
$\epsilon_{Ph_2^-}$ (dm^{3}mol^{-1}cm^{-1})	0	
$\epsilon_{(Mg^{II}, e_s^-)}$ (dm^{3}mol^{-1}cm^{-1})	$(4.1 \pm 0.1) \times 10^{4\ b}$	$(4.2 \pm 0.1) \times 10^4$

^{a} See Table 2 for notations. ^{b} Taken from ref 3. ^{c} See section III.1.a.
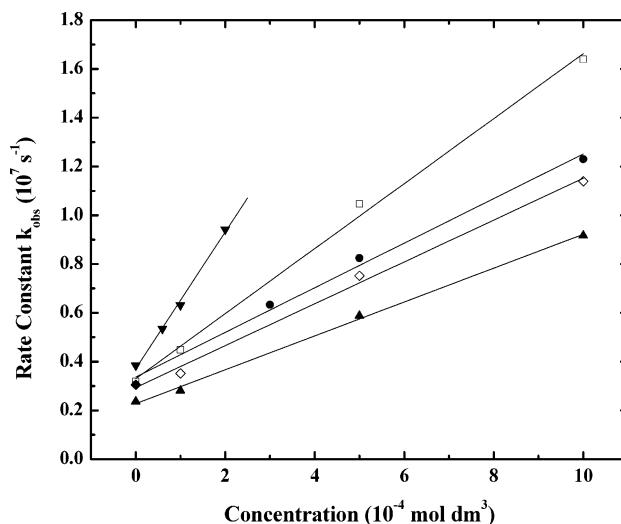

Figure 3. First-order rate constant, k_{obs}, of the optical change observed at 1000 nm as a function of the concentration of the aromatic compounds in THF solution containing 10^{-2} mol dm^{-3} of magnesium perchlorate: (▲) biphenyl, (◇) phenanthrene, (●) chrysene, (□) anthracene, and (▼) tetracene.

unknown: the rate constants k_{10}, k_{11}, k_{12}, and the extinction coefficient of the (Mg^{II}, Ph_2^-) pair at 1000 nm, $\epsilon_{(Mg^{II}, Ph_2^-)}$(1000). The best fit is obtained for $\epsilon_{(Mg^{II}, Ph_2^-)}$(1000) equal to zero but the rate constants k_{11} and k_{12} cannot be evaluated by that analysis. Consequently, the (Mg^{II}, Ph_2^-) pair does not absorb at 1000 nm. Such a result could be expected given the nature of the pair and the small spectral shift observed in the case of the (Na^+, Ph_2^-) pair.[18]

Therefore, as the (Mg^{II}, Ph_2^-) pair cannot be observed at 1000 nm, we can get rid of reactions 11 and 12 for the analysis of the signals at this wavelength. The simplified model is now identifiable and enables us to estimate the rate constant of the electron-transfer reaction between the pair and the biphenyl to be $k_{10} = (7.0 \pm 0.1) \times 10^9$ dm^3 mol^{-1} s^{-1} (Table 3). In parallel, we have evaluated k_{10} from the analysis of the pseudo-first-order decay of the pair, $k_{10} = (6.9 \pm 0.2) \times 10^9$ dm^3 mol^{-1} s^{-1} (Figure 3). There is again an excellent agreement between the pseudo-first order and full kinetic treatments. That confirms the proposed mechanism with the set of reactions and validates the simpler approach which will be retained for the analysis of the reactivity of (Mg^{II}, e_s^-) with other aromatic compounds.

The obtained k_{10} value is close to the reported value of the rate constant of the reaction between (Na^+, e_s^-) and biphenyl in THF $((5.5 \pm 0.1) \times 10^9$ dm^3 mol^{-1} s^{-1}).[1] The reaction rate constant found for the (Mg^{II}, e_s^-) pair with the biphenyl is roughly six times as low as that determined for the solvated

Reactivity of the (Mg^{II}, E$_s^-$) Pair

J. Phys. Chem. A, Vol. 107, No. 34, 2003 **6591**

electron ($k_7 = (3.9 \pm 0.1) \times 10^{10}$ dm^3 mol^{-1} s^{-1}). Slower reaction for the (Mg^{II}, e$_s^-$) pair compared to that of the solvated electron was also evoked to explain the decrease of the reduction rate of Zn^{2+} in ethanol solution in the presence of inert salts (Mg(ClO$_4$)$_2$ or Ca(ClO$_4$)$_2$).[19]

III.1.c. Reactivity of the (Mg^{II}, e$_s^-$) Pair with Other Aromatic Compounds. Similar pulse radiolysis experiments have been carried out to study the kinetics of the electron-transfer reaction from the (Mg^{II}, e$_s^-$) pair to other aromatic molecules: phenanthrene, chrysene, anthracene, and tetracene. The concentration of magnesium perchlorate at 10^{-2} mol dm^{-3} is in excess compared to the concentration of the organic solute (6×10^{-5} to 10^{-3} mol dm^{-3}), to ensure that in all the solutions the solvated electrons are mainly scavenged by Mg(ClO$_4$)$_2$ to produce the (Mg^{II}, e$_s^-$) pair. We follow the decay of the pair at 1000 nm versus the Ar concentration, which is much higher than the concentration of the pair produced by the pulse. In these conditions, we observe that the decay is accelerated by increasing the concentration of the aromatic compound and that there is no residual absorbance at the end of the decay at 1000 nm. This latter observation indicates that none of the radical anions (Ar$^-$) formed by electron attachment on the aromatic compounds (Ar) absorb at 1000 nm. Such a result is in agreement with the reported spectra of aromatic hydrocarbon mono-ions.[13,20] Consequently, the transient absorbance signal at 1000 nm is mainly due to the (Mg^{II}, e$_s^-$) pair. The measured decay at 1000 nm follows a pseudo-first-order law with an observed rate constant k_{obs}. From the linear fit of k_{obs} versus the Ar concentration (Figure 3), the rate constants k of the electron-transfer reaction from the pair to phenanthrene, chrysene, anthracene, and tetracene are found to be $(8.6 \pm 0.4) \times 10^9$, $(9.2 \pm 0.5) \times 10^9$, $(1.3 \pm 0.1) \times 10^{10}$, and $(2.8 \pm 0.1) \times 10^{10}$ dm^3 mol^{-1} s^{-1}, respectively (Table 1). The values obtained in the present work for reduction of aromatic hydrocarbons by the (Mg^{II}, e$_s^-$) pair are an order of magnitude lower than that reported for the reduction of similar aromatic hydrocarbons by solvated electron in THF[12,21] and are close to the values reported for the reduction by (Na$^+$, e$_s^-$) pair.[1,17]

Figure 4 presents the obtained rate constants as a function of the redox potential of the Ar/Ar$^-$ couple. We remark that the electron-transfer reaction increases with the reduction potential. As the electron transfer corresponds to a bimolecular reaction, the rate constant includes the electron-transfer term itself (k_{et}) but also a diffusion part (k_{diff})

$$\frac{1}{k} = \frac{1}{k_{diff}} + \frac{1}{k_{et}} \quad (13)$$

According to the classical Marcus theory, k_{et} is given by

$$k_{et} = Z \exp\left[-\frac{\lambda}{4N_A k_B T}\left(1 + \frac{\Delta G^\circ}{\lambda}\right)^2\right] \quad (14)$$

where N_A is the Avogadro constant, k_B is the Boltzman constant, T is the temperature, Z represents the collision frequency with an electron transfer, λ denotes the solvent reorganization energy, and ΔG° is the standard Gibbs energy of the reaction.

We can evaluate k_{diff} using the Smoluchowski's equation

$$k_{diff} = 4\pi DR \quad (15)$$

where D corresponds to the mutual diffusion constants of the two reactants and R is the mean separation distance between the two reactants. As the half-thickness of a planar aromatic is around 2.5 Å and the radius of the pair close to 5 Å (estimated
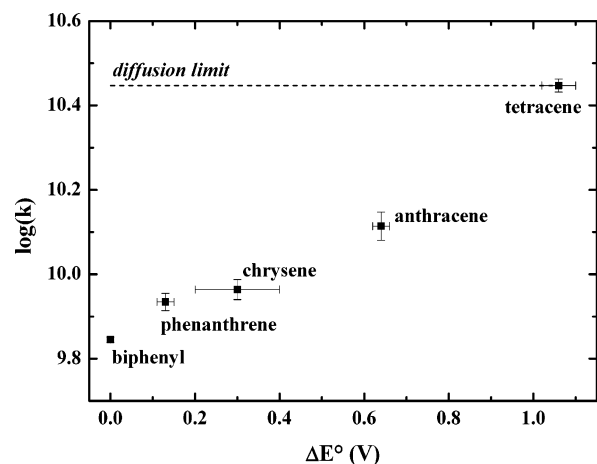

Figure 4. Plot of log(k) for the electron-transfer reaction between the (Mg^{II}, e$_s^-$) pair and aromatic compounds as a function of the reduction potential of the aromatic compounds (Table 1). The dotted line represents the estimated diffusion limit k_{diff} (see text).

from the geometry of the pair derived by quantum chemistry calculations[3]), R is taken equal to 7.5 Å. The diffusion constants of the studied hydrocarbons in THF have close values because the mobility of the molecule is mostly determined by the area of the smallest cross-section perpendicular to the plane of the molecule. For instance, the values of the diffusion constant for biphenyl and anthracene are 2.4×10^{-5} cm^2 s^{-1} and 2×10^{-5} cm^2 s^{-1}, respectively.[18] For the unknown diffusion constant of the pair, we assume a similar value. Hence, we obtain for the mutual diffusion constant: $D \approx 5 \times 10^{-5}$ cm^2 s^{-1}. Thereby, we find $k_{diff} \approx 2.8 \times 10^{10}$ dm^3 mol^{-1} s^{-1}, which is reasonable value compared to the estimated value of the diffusion controlled rate constant for the solvated electron in THF ($k_{diff} \approx 1.7 \times 10^{11}$ dm^3 mol^{-1} s^{-1}).[12]

As the Gibbs energy of the electron transfer reaction is linearly related to the redox potentials of the reactants

$$\Delta G^\circ = F[E^\circ((Mg^{II}/(Mg^{II}, e_s^-)) - E^\circ(Ar/Ar^-)] \quad (16)$$

with F the Faraday constant, the observed behavior is in agreement with the classical Marcus theory in the normal region. Note that in eq 16 we consider that the radical anions are not paired with Mg^{II}. The approximation is due to the lack of data concerning the nature of the formed species and the redox potential of Ar$^-$ paired with Mg^{II}. Nevertheless, we can assume that the trends of the redox potentials are similar. The rate constant k of the reduction of the aromatic compound by the pair increases with increasing $E^\circ(Ar/Ar^-)$ when $k_{diff} > k_{act}$ before reaching the diffusion limit for $k_{diff} \approx k_{act}$ (Figure 4). The lowest rate constant $((7.0 \pm 0.1) \times 10^9$ dm^3 mol^{-1} s$^{-1})$ corresponds to the electron-transfer reaction toward biphenyl whose reduction potential is the lowest, whereas the highest reaction rate constant $((2.8 \pm 0.1) \times 10^{10}$ dm^3 mol^{-1} s$^{-1})$ is associated to tetracene with the highest reduction potential. Because the electron-transfer reaction takes place with biphenyl, the redox potential of the pair must be lower than that of biphenyl. Nevertheless, as we have pointed out above, the rate of the electron-transfer reaction for the (Mg^{II}, e$_s^-$) pair is slower than that for the solvated electron; thereby, we can deduce that the redox potential of the pair is higher than that of the solvated electron. Hence, the following relation can be written

$$E^\circ(THF/e_s^-) < E^\circ(Mg^{II}/(Mg^{II}, e_s^-)) < E^\circ(Ph_2/Ph_2^-) \quad (17)$$

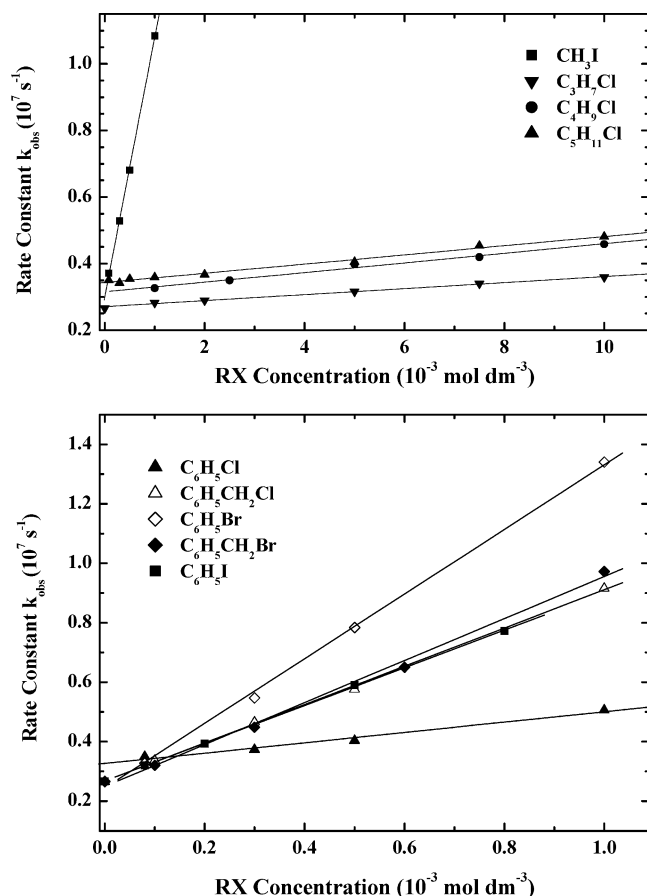So, the (Mg^{II}, e$_s^-$) pair is a less reducing species than the

Figure 5. First-order rate constant, k_{obs}, of the optical change observed at 1000 nm as a function of the RX concentration in THF solution containing 10^{-2} mol dm^{-3} of magnesium perchlorate.

solvated electron. The presence of the metal cation in the vicinity of the solvated electron, which acts as a trap and shields the interaction between the reactants, diminishes the reducing properties of the solvated electron.

III.2. Reactivity with Halogenated Hydrocarbon Compounds. To study the electron-transfer reaction from the (Mg^{II}, e$_s^-$) pair to alkyl halogens RX (reaction 18), we have achieved pulse radiolysis experiments with THF solutions containing magnesium perchlorate (10^{-2} mol dm^{-3}) and one RX compound (6×10^{-5} to 10^{-3} mol dm^{-3} for C$_6$H$_5$Cl, C$_6$H$_5$Br, C$_6$H$_5$I, C$_6$H$_5$CH$_2$Cl, C$_6$H$_5$CH$_2$Br, and CH$_3$I and 10^{-3} to 10^{-2} mol dm^{-3} for C$_3$H$_7$Cl, C$_4$H$_9$Cl, and C$_5$H$_{11}$Cl because those species react very slowly)

$$(Mg^{II}, e_s^-) + RX \rightarrow R^\bullet + X^- + Mg^{II} \qquad (18)$$
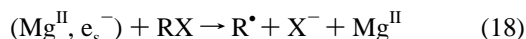
Under those conditions, the solvated electron reacts mostly with the magnesium salt to form the (Mg^{II}, e$_s^-$) pair within the electron pulse duration. We observe that the decay of the pair at 1000 nm is accelerated by increasing the concentration of RX (Figure 5). As the RX concentrations are much higher than the pair concentration produced in the pulse (around 10^{-5} mol dm^{-3}),[3] the decay is ruled by reaction 18 and obeys pseudo-first-order kinetics with an observed rate constant k_{obs} (Figure 5 inset). The linear dependence of k_{obs} versus RX concentration enables us to determine the rate constants of reaction 18 (Figure 5). The results are reported in Table 4. We remark that the rate constants obtained for the linear alkyl halogens are lower than those estimated for the phenyl and benzyl ones. A similar trend is reported for the reactivity of the solvated electron in THF

TABLE 4: Rate Constant of the Reaction between the (Mg^{II}, E$_s^-$) Pair and Various RX Molecules in THF

RX group	Compound	Formula	k (dm^3 mol^{-1} s^{-1})
phenyl	Chlorobenzene	C$_6$H$_5$Cl	$(1.7 \pm 0.2) \times 10^9$
	Bromobenzene	C$_6$H$_5$Br	$(7.1 \pm 0.3) \times 10^9$
	Iodobenzene	C$_6$H$_5$I	$(6.3 \pm 0.1) \times 10^9$
benzyl	Chloromethylbenzene	C$_6$H$_5$CH$_2$Cl	$(6.4 \pm 0.1) \times 10^9$
	Bromomethylbenzene	C$_6$H$_5$CH$_2$Br	$(1.1 \pm 0.1) \times 10^{10}$
	Iodomethane	CH$_3$I	$(7.8 \pm 0.2) \times 10^9$
Linear alkyl	1-chloropropane	C$_3$H$_7$Cl	$(9.1 \pm 0.3) \times 10^7$
CH$_3$–(CH$_2$)$_n$–X	1-chlorobutane	C$_4$H$_9$Cl	$(1.4 \pm 0.1) \times 10^9$
	1-chloropentane	C$_5$H$_{11}$Cl	$(1.4 \pm 0.1) \times 10^9$

but with larger values. For example, the rate constant value reported for the reaction between the benzyl chloride and solvated electron ($k = (10.03 \pm 0.04) \times 10^{10}$ dm^3 mol^{-1} s^{-1})[12] is more than 1 order of magnitude higher than our estimated value for the (Mg^{II}, e$_s^-$) pair ($k = (6.4 \pm 0.1) \times 10^9$ dm^3 mol^{-1} s^{-1}). In addition, for the aromatics series, we note that the nature of the halogen influences the reactivity: Cl is less reactive than Br and I, in accord with the reported increase in the reduction potentials from chloro to bromo derivatives.[22] Lower rate constant values for the reaction between the solvated electron (or the (Na$^+$, e$_s^-$) pair) and n-butyl bromide compared with n-butyl iodide have already been reported.[1] Those results are consistent with those reported for the reaction between halobenzenes and solvated electrons in liquid ammonia.[23]

IV. Conclusion

In this companion contribution of a previously published work,[3] we have studied the reactivity of the (Mg^{II}, e$_s^-$) pair formed by the solvated electron and the magnesium perchlorate in THF solution.

First, we have carried out experiments in the presence of aromatic compounds with different reduction potentials. As a first step, we have focused on the reaction of the pair with biphenyl. We have optimized our experimental conditions to avoid the direct reaction of the solvated electron with the aromatic compound. We have measured the rate constant of the reaction between solvated electron and biphenyl (($3.9 \pm 0.1) \times 10^{10}$ dm^3 mol^{-1} s^{-1}). Then, the rate constant of the reaction between (Mg^{II}, e$_s^-$) and biphenyl has been determined to be equal to $(7.0 \pm 0.1) \times 10^9$ dm^3 mol^{-1} s^{-1}. Afterward, the rate constants of the electron-transfer reaction from the pair toward various aromatic compounds have been evaluated. They increase with the reduction potential of the aromatic molecule but stay lower than the diffusion-limited rate constant.

Second, we have observed the reaction of the pair toward nine halogenated hydrocarbons. The reaction rate constants have been determined, ranging from 9.1×10^7 to 1.1×10^{10} dm^3 mol^{-1} s^{-1}. The lowest and highest values correspond to linear alkyl and benzyl compounds, respectively, whereas the intermediates values are related to phenyl halogens.

Finally, this set of results indicates that the pair is a reducing species because it can reduce even biphenyl, which is known to have a low redox potential, but it is a less reducing agent than the solvated electron. Moreover, the (Mg^{II}, e$_s^-$) pair appears as a quite reactive species. Consequently, if we consider (Mg^{II}, e$_s^-$) as a pseudo-monovalent magnesium intermediate in the oxidation processes of the magnesium metal powder involved in the dehalogenation of hydrocarbon compounds or in the

Reactivity of the (Mg^{II}, E$_s^-$) Pair

J. Phys. Chem. A, Vol. 107, No. 34, 2003 **6593**

formation of Grignard reagents in solution, we may conclude that the kinetics of the subsequent electron transfer from the pseudomonovalent magnesium to the solute are very fast.

References and Notes

(1) Bockrath, B.; Dorfman, L. M. *J. Phys. Chem.* **1973**, *77*, 1002. Fletcher, J. W.; Seddon, W. A. *J. Phys. Chem.* **1975**, *79*, 3055.

(2) Salmon, G. A.; Seddon, W. A.; Fletcher, J. W. *Can. J. Chem.* **1974**, *52*, 3259. Fletcher, J. W.; Seddon, W. A. *J. Phys. Chem.* **1975**, *79*, 3055.

(3) Renou, F.; Mostafavi, M.; Archirel, P.; Bonazzola, L.; Pernot, P. *J. Phys. Chem. A* **2003**, *107*, 1506.

(4) Renou, F.; Mostafavi, M. *Chem. Phys. Lett.* **2001**, *335*, 363.

(5) Mackenzie, K.; Kopinke, F.-D.; Remmler, M. *Chemosphere* **1996**, *33*, 1495. Sun, G.-R.; He, J.-B.; Pittman, C. U., Jr. *Chemosphere* **2000**, *41*, 907.

(6) Wang, T. C.; Tan, C. K. *Bull. Environ. Contam. Toxicol.* **1990**, *45*, 149.

(7) Garst, J.; Hungvary, F. In *Grignard reagents. New developments*; Richey, H. G., Ed.; J. Wiley: New York, 2000.

(8) Belloni, J.; Billiau, F.; Cordier, P.; Delaire, J.; Delcourt, M. O. *J. Phys. Chem.* **1978**, *82*, 532.

(9) Sivia, D. S. *Data Analysis: A Bayesian Tutorial*; Clarendon: Oxford, 1996.

(10) Gilks, W. R.; Richardson, S.; Spiegelhalter, D. J. *Markov Chain Monte Carlo in Practice*; Chapman and Hall: London, 1996.

(11) Petzold, L. R. *Siam J. Sci. Stat. Comput.* **1983**, *4*, 136.

(12) Kadhum, A. A. H; Salmon, G. A. *J. Chem. Soc., Faraday Trans. I* **1986**, *82*, 2521.

(13) Jagur-Grodzinski, J.; Feld, M.; Yang, S. L.; Szwarc, M. *J. Phys. Chem.* **1965**, *69*, 628.

(14) Hunt, J. W. *Adv. Radiat. Chem.* **1976**, *5*, 85. Fendler, J. H.; Gillis, H. A.; Klassen, N. V. *J. Chem. Soc., Faraday Trans. I* **1974**, *70*, 145.

(15) Dorfman, L. M.; Jou, F. Y.; Wageman, R. *Ber. Buns. Phys. Chem.* **1971**, *75*, 681.

(16) Private communication: unpublished pulse radiolysis results obtained by J. Miller and co-workers at the Brookhaven National Laboratory (U.S.A.).

(17) Fisher, M.; Ramme, G.; Claesson, S.; Scwarc, M. *Chem. Phys. Lett.* **1971**, *9*, 306.

(18) Chang, P.; Slates, R. V.; Szwarc, M. *J. Phys. Chem.* **1966**, *70*, 3180.

(19) Hickel, B. *J. Phys. Chem.* **1978**, *82*, 1005.

(20) Hoijtink, G. J.; Zandstra, P. J. *Mol. Phys.* **1960**, *3*, 371. *UV Atlas of organic compounds*; Perkampus, H. H.; Sanderman, I; Timmons, C. J., Eds.; Butterworths, Verlag Chemie: London, 1966.

(21) Jou, F. Y.; Dorfman, L. M. *J. Chem. Phys.* **1973**, *58*, 4715.

(22) Andrieux, C. P.; Blocman, C.; Dumas-Bouchiat, J.-M.; Saveant, J.-M. *J. Am. Chem. Soc.* **1979**, *101*, 3431.

(23) Andrieux, C. P.; Saveant, J.-M. *J. Am. Chem. Soc.* **1993**, *115*, 8044.

(24) Perichon, J.; Buvet, R. *Bull. Soc. Chim.* **1968**, *3*, 1282. Slates, R. V.; Swarcz, M. *J. Phys. Chem.* **1965**, *69*, 4124.

(25) Hoitjink, G. J.; De Boer, E.; van der Meij, P. H.; Weijland, W. P. *Rec. Trav. Chim. Pays-Bas* **1956**, *75*, 487.